

## Characterization of the New n\_TOF Neutron Beam: Fluence, Profile and Resolution

C. GUERRERO,<sup>1,\*</sup> V. BECARES,<sup>1</sup> D. CANO-OTT,<sup>1</sup> M. FERNANDEZ-ORDONEZ,<sup>1</sup> E. GONZALEZ-ROMERO,<sup>1</sup> F. MARTIN-FUERTE,<sup>1</sup> T. MARTINEZ,<sup>1</sup> E. MENDOZA,<sup>1</sup> G. PINA,<sup>1</sup> J. QUINONES,<sup>1</sup> V. VLACHOUDIS,<sup>1</sup> M. CALVIANI,<sup>2</sup> S. ANDRIAMONJE,<sup>2</sup> M. BRUGGER,<sup>2</sup> F. CERUTTI,<sup>2</sup> E. CHIAVERI,<sup>2</sup> A. FERRARI,<sup>2</sup> Y. KADI,<sup>2</sup> E. LEBBOS,<sup>2</sup> E. BERTHOUMIEUX,<sup>3</sup> F. GUNSING,<sup>3</sup> J. ANDRZEJEWSKI,<sup>4</sup> J. MARGANIEC,<sup>4</sup> J. PERKOWSKI,<sup>4</sup> L. AUDOUIN,<sup>5</sup> B. BERTHIER,<sup>5</sup> L. TASSAN-GOT,<sup>5</sup> V. AVRIGEANU,<sup>6</sup> M. MIREA,<sup>6</sup> F. BECVAR,<sup>7</sup> M. KRICKA,<sup>7</sup> F. BELLONI,<sup>8</sup> P. M. MILAZZO,<sup>8</sup> F. CALVINO,<sup>9</sup> G. CORTES,<sup>9</sup> M. B. GOMEZ-HORNILLOS,<sup>9</sup> C. CARRAPICO,<sup>10</sup> I. F. GONCALVES,<sup>10</sup> R. SARMENTO,<sup>10</sup> P. VAZ,<sup>10</sup> N. COLONNA,<sup>11</sup> S. MARRONE,<sup>11</sup> M. MOINUL,<sup>11</sup> G. TAGLIENTE,<sup>11</sup> V. VARIALE,<sup>11</sup> I. DILLMANN,<sup>12</sup> C. DOMINGO-PARDO,<sup>13</sup> M. HEIL,<sup>13</sup> I. DURAN,<sup>14</sup> C. PARADELA,<sup>14</sup> D. TARRIO,<sup>14</sup> S. GANESAN,<sup>15</sup> G. GIUBRONE,<sup>16</sup> J. L. TAIN,<sup>16</sup> F. GRAMEGNA,<sup>17</sup> P. F. MASTINU,<sup>17</sup> S. HARRISOPULOS,<sup>18</sup> K. IOANNIDES,<sup>19</sup> D. KARADIMOS,<sup>19</sup> E. JERICHA,<sup>20</sup> H. LEEB,<sup>20</sup> C. WEISS,<sup>20</sup> F. KÄPPELER,<sup>21</sup> C. LEDERER,<sup>22</sup> A. PAVLIK,<sup>22</sup> A. WALLNER,<sup>22</sup> M. LOZANO,<sup>23</sup> J. PRAENA,<sup>23</sup> J. M. QUESADA,<sup>23</sup> C. MASSIMI,<sup>24</sup> G. VANNINI,<sup>24</sup> A. MENGONI,<sup>25</sup> A. VENTURA,<sup>25</sup> M. MOSCONI,<sup>26</sup> R. NOLTE,<sup>26</sup> and R. VLASTOU<sup>27</sup>

(The n\_TOF Collaboration ([www.cern.ch/n\\_TOF](http://www.cern.ch/n_TOF)))

<sup>1</sup>Centro de Investigaciones Energeticas, Medioambientales y Tecnologicas, Madrid, 28040, Spain

<sup>2</sup>CERN, Geneva, Switzerland

<sup>3</sup>CEA/Saclay - Irfu/SPhN, Gif-sur-Yvette, France

<sup>4</sup>University of Lodz, Lodz, Poland

<sup>5</sup>Centre National de la Recherche Scientifique/IN2P3-IPN, Orsay, France

<sup>6</sup>Horia Hulubei National Institute of Physics and Nuclear Engineering-IFIN HH, Bucharest-Magurele, Romania

<sup>7</sup>Faculty of Mathematics and Physics, Charles University, Prague, Czech Republic

<sup>8</sup>Istituto Nazionale di Fisica Nucleare, Trieste, Italy

<sup>9</sup>Universitat Politecnica de Catalunya, Barcelona, Spain

<sup>10</sup>Instituto Tecnol6gico e Nuclear (ITN), Lisbon, Portugal

<sup>11</sup>Istituto Nazionale di Fisica Nucleare, Bari, Italy

<sup>12</sup>Physik Department E12, Technische Universitat Munchen, and Excellence Cluster Universe, Garching, Germany

<sup>13</sup>GSI Helmholtzzentrum ur Schwerionenforschung GmbH, Darmstadt, Germany

<sup>14</sup>Universidade de Santiago de Compostela, Spain

<sup>15</sup>BARC, Mumbai, India

<sup>16</sup>Instituto de Fisica Corpuscular, CSIC-Universidad de Valencia, Spain

<sup>17</sup>Istituto Nazionale di Fisica Nucleare, Laboratori Nazionali di Legnaro, Italy

<sup>18</sup>NCSR, Demokritos, Greece

<sup>19</sup>University of Ioannina, Greece

<sup>20</sup>Atominstytut der 6sterreichischen Universitaten, Technische Universitat Wien, Austria

<sup>21</sup>Karlsruhe Institute of Technology, Campus Nord,

, Institut fur Kernphysik, 76021 Karlsruhe, Germany

<sup>22</sup>VERA Laboratory, Faculty of Physics, University of Vienna, Vienna 1090, Austria

<sup>23</sup>Universidad de Sevilla, Spain

<sup>24</sup>Dipartimento di Fisica, Universita di Bologna, and Sezione INFN di Bologna, Italy

<sup>25</sup>ENEA, Bologna, Italy

<sup>26</sup>Physikalisch-Technische Bundesanstalt (PTB), Braunschweig, Germany

<sup>27</sup>National Technical University of Athens, Greece

(Received 26 April 2010)

After a halt of four years, the n\_TOF spallation neutron facility at CERN has resumed operation in November 2008 with a new spallation target characterized by an improved safety and engineering design, resulting in a more robust overall performance and efficient cooling.

The first measurement during the 2009 run has aimed at the full characterization of the neutron beam. Several detectors, such as calibrated fission chambers, the n\_TOF Silicon Monitor, a MicroMegs detector with <sup>10</sup>B and <sup>235</sup>U samples, as well as liquid and solid scintillators have been used in order to characterize the properties of the neutron fluence. The spatial profile of the beam has been studied with a specially designed “X-Y” MicroMegs which provided a 2D image of the beam

as a function of neutron energy. Both properties have been compared with simulations performed with the FLUKA code. The characterization of the resolution function is based on results from simulations which have been verified by the study of narrow capture resonances of  $^{56}\text{Fe}$ , which were measured as part of a new campaign of  $(n,\gamma)$  measurements on Fe and Ni isotopes.

PACS numbers: 28.20.-v, 29.27.-a

Keywords: n\_TOF, Time-of-flight, Neutron beam, Nuclear data, Cross sections

DOI: 10.3938/jkps.59.1624

## I. INTRODUCTION

The neutron time-of-flight facility n\_TOF [1] at CERN has been devoted, from its construction in 1998-2001, to the measurement of neutron capture and fission cross sections of isotopes relevant for innovative nuclear technologies as well as for nuclear astrophysics. The uniqueness of this facility resides in the combination of a very high instantaneous flux ( $10^6$  neutrons/pulse from  $1 - 10^6$  eV) at a long flight-path (185 m) with state of the art detectors and data acquisition systems. Further references about the facility and the main results obtained during the Phase-1 (2002 – 2004) are given elsewhere [2].

The facility has recently resumed operation after a halt of four years during which a new and optimized spallation target has been constructed and installed.

This contribution describes briefly the new target and the measurements carried out during 2009 for the commissioning of the new spallation target, summarizing the main results. These regard the intensity and energy distribution of the neutron flux, the profile of the neutron beam at the measuring station and the energy resolution of the neutron beam.

## II. THE NEW SPALLATION TARGET

Neutrons at n\_TOF are generated by spallation reactions produced by protons of 20 GeV from the CERN PS on a lead target. The new spallation target of the n\_TOF facility, sketched in Fig. 1, is basically a cylindrical lead block 40 cm in length and 60 cm in diameter. Besides the shape of the lead block, the main difference with respect to the previous n\_TOF target is the separation of the circuits for cooling and moderation.

The cooling circuit consists of a water layer of 1 cm that surrounds the target, while the moderation circuit is a 4 cm thick vessel that can be filled with either water or borated water. In the latter case most thermal neutrons are absorbed by means of  $^{10}\text{B}(n,\alpha)$  reactions, hence suppressing the 2.2 MeV  $\gamma$ -ray background from  $^1\text{H}(n,\gamma)$  reactions which in the past has been the main source of background in measurements with  $\text{C}_6\text{D}_6$  detectors [6].

Table 1. Measurements for the characterization of the n\_TOF neutron flux.

Detector	Reaction	Energy range (eV)	Refs.
PTB	$^{235}\text{U}(n,f)$	$10^{-2} - 10^7$	[3]
MGAS	$^{235}\text{U}(n,f)$	$10^{-2} - 10^5$	[4]
MGAS	$^{10}\text{B}(n,\alpha)$	$10^{-2} - 10^4$	[4]
SiMon	$^6\text{Li}(n,\alpha)$	$10^{-2} - 10^3$	[5]

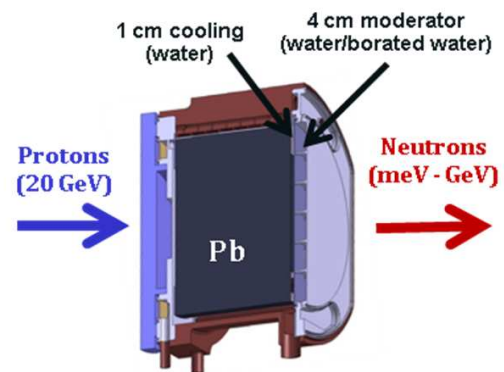


Fig. 1. (Color online) Sketch of the new lead spallation target. Note the independent circuits for cooling (water) and moderation (water or borated water).

## III. NEUTRON FLUX

The 2009 experimental campaign made use of a water moderator and hence the following results correspond to that configuration. The absolute intensity and distribution of the neutron flux as function of energy have been determined in four different measurements, which are summarized in Table 1.

The PTB detector [3] is a well calibrated and certified fission chamber containing five  $^{235}\text{U}$  samples with a total mass of 201.4 (5) mg. The MicroMegas (MGAS) [4] detector, based on the microbulk technology, is a transparent charged-particle detector built by the n\_TOF Collaboration for continuous monitoring of the neutron flux during the cross section measurements. Last, the Silicon Monitor (SiMon) [5] is the primary n\_TOF monitor, consisting of 4 silicon detectors looking at a  $^6\text{Li}$  target.

The highest accuracy is provided by the PTB fission chamber and determines the absolute intensity of the flux. However, neutron capture cross sections are measured relative to some reference and hence the energy dependence of the neutron flux is more important than

\*E-mail: carlos.guerrero@ciemat.es

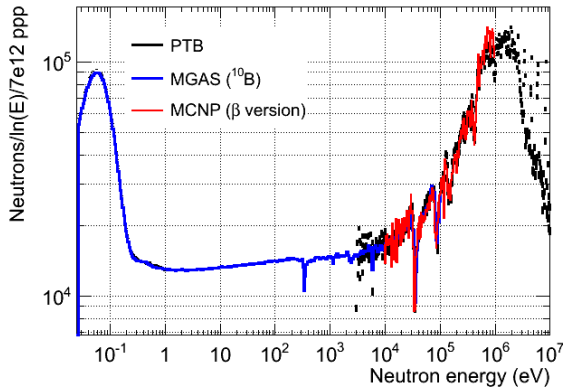


Fig. 2. (Color online) Neutron flux from the PTB fission chamber and the MGAS ( $^{10}\text{B}$ ) together with the MCNP simulations used to characterize the dips in the flux.

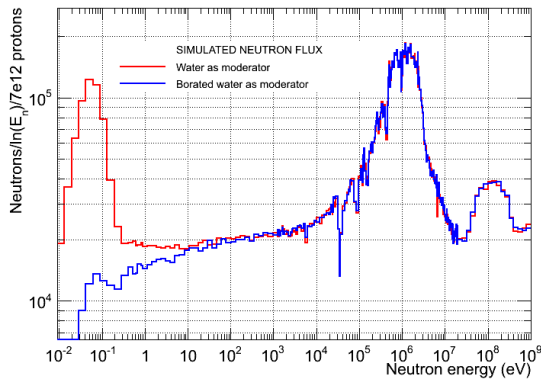


Fig. 3. (Color online) The use of borated water as a moderator will reduce the background of in-beam  $\gamma$ -rays, but affects also the neutron flux in the region below 10 eV.

the absolute flux. For that reason, the flux has been measured with different detectors based on different reactions in order to minimize the uncertainty on the energy dependence.

The results, after normalizing all data to the PTB results in the region 0.1 to 1 eV, are shown in Fig. 2. The flux is dominated by the evaporation peak in the MeV region, a nearly isoenergic distribution between 1 eV and several hundred keV, and a thermal peak in the meV region. The dips in the keV region are transmission dips from the aluminium windows along the beam line.

All results are in good agreement, and are well reproduced by MCNP and FLUKA simulations with ENDF/B-VII. The combination of all the measured and simulated (unlimited statistics) results provides the so-called evaluated neutron flux that is used for the analysis of cross sections. The uncertainty in the energy distribution of this evaluated flux is only 2%, which corresponds to the degree of agreement between experimental data. The simulations serve to describe with narrow bins the fluence in the dips observed at 0.01 – 1 MeV.

Table 2. Beam interception factor for different sample radii as function of neutron energy.

Sample radius (mm)	Neutron energy range (eV)						
	$10^{-2}$	1	10	$10^2$	$10^3$	$10^4$	$10^5$
5	0.153	0.159	0.161	0.162	0.165	0.166	0.173
10	0.501	0.513	0.519	0.522	0.528	0.530	0.546
15	0.815	0.822	0.828	0.832	0.835	0.836	0.846
20	0.975	0.976	0.977	0.979	0.979	0.979	0.981

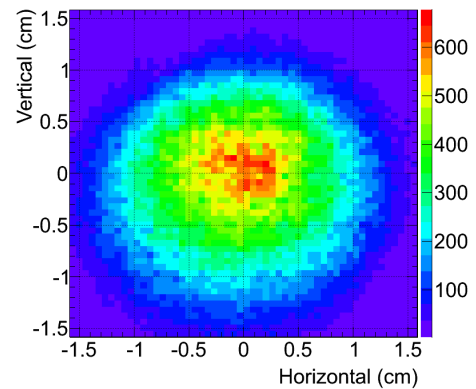


Fig. 4. (Color online) 2D profile of the neutron beam measured with the XY-MicroMegas at thermal neutron energy.

The use of borated water as a moderator starting from 2010 will lead to a change in the neutron flux, mainly at low energies. The advantage is that the intensity of in-beam  $\gamma$ -rays flying along with the neutrons will be highly reduced, ensuring lower background in capture measurements with  $\text{C}_6\text{D}_6$  detectors [6]. The calculations, displayed in Fig. 3, indicate that the neutron flux will remain unchanged above 10 eV while the background of 2.2 MeV  $\gamma$ -rays will be reduced by at least an order of magnitude.

#### IV. BEAM PROFILE

The characterization of the beam profile is of primary importance because in most neutron capture measurements the samples are smaller than the neutron beam. This allows one to reduce uncertainties related to inhomogeneities of the samples and to maximize the reaction yield, but implies that corrections must be made according to the fraction of beam intercepted by the sample, which may depend on neutron energy.

A new detector, the *X-Y MicroMegas* (XYMG) [7], was developed for the determination of the beam profile. Also based in the bulk technology, it consisted of a  $6 \times 6 \text{ cm}^2$  active area subdivided into  $106 \times 106$  strips read by two 96 channels Gassiplex cards. With this resolution the beam profile could be determined at any neutron energy. A  $^{10}\text{B}$  converter has been used with two different

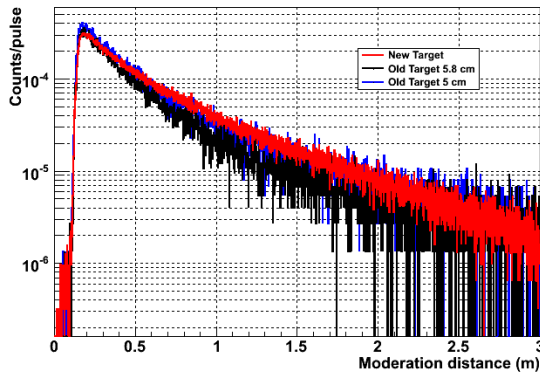


Fig. 5. (Color online) Resolution Function, expressed as moderation distance, of the new and old spallation target in the region around 100 keV, where the resolution broadening becomes dominant.

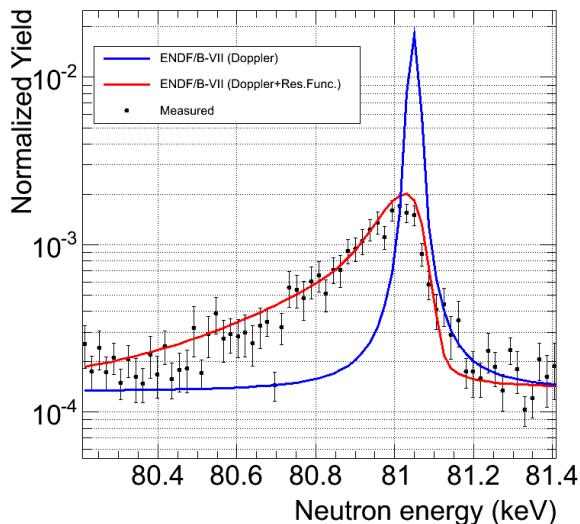


Fig. 6. (Color online) The measured  $^{56}\text{Fe}(n,\gamma)$  resonance near 81 keV and the expected shape with and without broadening by the RF.

thicknesses: 20 nm to investigate low neutron energy range, and 2  $\mu\text{m}$  to study the profile for neutron energies up to 1 MeV.

The beam profile for thermal neutrons is shown in Fig. 4. The collimation system along the beam line provides a nearly Gaussian profile with a width of  $\sim 7$  mm changing slightly with neutron energy. Hence, the fraction of the beam intercepted by sample of a given size varies slightly with energy as shown in Table 2.

## V. RESOLUTION FUNCTION

Due to the finite width of the proton pulse and due to the neutron production and moderation processes, neutrons of the same energy leave the target at different

times. The function relating the time-of-flight with the energy of the neutrons is referred to as Resolution Function (RF), and becomes the dominating broadening effect (over Doppler) at energies above some tens of keV.

The RF of the new target has been determined from simulations and is described analytically by a modified RPI function, see [8]. Above 100 keV (see Fig. 5), the RF of the new target is essentially similar to that of the previous target [7]. At lower energies, the tail of the distributions is broadened due to the effect of the air gap between the exit of the target and the beginning of the TOF tube.

The correctness of the analytical function is tested by comparison of the expected with the measured shape for narrow resonances which width are dominated by the resolution broadening. This is illustrated in Fig. 6, where the expected and measured shapes are in excellent agreement. The magnitude of the RF broadening with respect to Doppler is illustrated by the large difference in the width of the blue and red lines (with and without including the RF broadening).

## ACKNOWLEDGMENTS

The restart of the n\_TOF facility would not have been possible without the contribution of many people, in particular without the technical support from Y. Body, R. Mollay, P. Carbonez, J. Lendaro, M. Lazzaroni, T. Otto, D. Grenier, S. Girod, S. Sgobba, L. Marques Ferreira and D. Duarte Ramos.

This work was partially supported by Spanish FPA2008-06419-C02-01, FPA2005-06918-C03-01 and CSD-2007-00042, and grants by ENRESA under the CIEMAT-ENRESA agreement on “Transmutation of high level radioactive waste”, by the European Commission 6th Framework Programme project IP-EUROTRANS (FI6W-CT-2004-516520), the European Commission transnational access program EFNUDAT and by the Austrian Science Fund (FWF) [P20434].

## REFERENCES

- [1] F. Gunsing *et al.*, Nucl. Instrum. Methods Phys. Res. Sect. B **261**, 925 (2007).
- [2] N. Colonna *et al.*, Appl. Radiat. Isotopes **68**, 643 (2010).
- [3] D. B. Gayther, Metrologia **27**, 221 (1990).
- [4] S. Andriamonje *et al.*, *Inter. Conf. on Nucl. Data for Sci. and Techn.-ND2010* (Jeju, Korea, 2010).
- [5] S. Marrone *et al.*, Nucl. Instrum. Methods Phys. Res. Sect. A **517**, 389 (2004).
- [6] C. Domingo-Pardo *et al.*, Phys. Rev. C **75**, 045805 (2007).
- [7] S. Andriamonje *et al.*, *Inter. Conf. on Nucl. Data for Sci. and Techn.-ND2010* (Jeju, Korea, 2010).
- [8] C. Coceva *et al.*, Nucl. Instrum. Methods Phys. Res. Sect. A **489**, 346 (2002).